Electronic Supplementary Material (ESI) for ChemComm.

Complete Switch from α2,3- to α2,6-Regioselectivity in *Pasteurella dagmatis* β-D-Galactoside Sialyltransferase by Active-Site Redesign

Supporting Information

Katharina Schmölzer,[a] Tibor Czabany,[b] Christiane Luley-Goedl,[a] Tea Pavkov-Keller,[a] Doris Ribitsch,[a] Helmut Schwab,[c] Karl Gruber,[d] Hansjörg Weber,[e] and Bernd Nidetzky*[ab]

[a] *Austrian Centre of Industrial Biotechnology, Petersgasse 14, 8010 Graz, Austria.*
[b] *Institute of Biotechnology and Biochemical Engineering, Graz University of Technology, Petersgasse 12/1, 8010 Graz, Austria.*
E-mail: bernd.nidetzky@tugraz.at; Fax: +43 316 8738434; Tel: +43 316 8738400
[c] *Institute of Molecular Biotechnology Graz, University of Technology, Petersgasse 14, 8010 Graz, Austria.*
[d] *Institute of Molecular Biosciences, University of Graz, Humboldtstrasse 50/3, 8010 Graz, Austria.*
[e] *Institute of Organic Chemistry, Graz University of Technology, Stremayrgasse 9, 8010 Graz, Austria.*

Table of contents

Materials and methods

Chemicals

Ampicillin, IPTG, imidazole, BSA and acetonitrile were from Carl-Roth (Austria). CMP-Neu5Ac and lactose were obtained from Sigma-Aldrich (Austria) in the highest purity available. Moreover, tetrabutylammonium hydrogen sulfate, NaOH solution (50% in H2O) and sodium acetate in the HPLC grade were also from Sigma-Aldrich. PNGase F, α2,3-neuraminidase and neuraminidase were from New England Biolabs (Germany). 2-nitrophenyl-β-D-galactopyranoside (oNP-βGal), *N*-acetyllactosamine, 3'- and 6'-sialyllactose sodium salt and 3'- and 6'-sialyl-*N*-acetyllactosamine were from Carbosynth (UK).

Site-directed mutagenesis

Mutations to replace Pro^{7} by His (P7H) and Met^{117} by Ala (P7H-M117A) were introduced by two-stage PCR[1] where a pET23a(+) expression vector encoding ∇3PdST (variant of wild-type PdST elongated by three amino acids at the N-terminus)[2] was used as a template. A pair of complementary oligonucleotide primers, each introducing the desired site-directed substitution at the protein level, was used. The mismatched bases are underlined.

P7H forward:

5'-ATACATATGAAAACAATCACAATCTATTTAGATCATGCTTCATTACCCACATTA AACCAATTAATGCAC-3'

P7H reverse:

5'-GTGCATTAATTGGTTTAATGTGGGTAATGAAGCATGATCTAAATAGATTGTGA TTGTTTTCATATGTAT-3'

M117A forward:

5'-CTTTATGATGATGGCACAGCGGAATATGTTGATTTAG-3'

M117A reverse:

5'-CTAAATCAACATATTCCGCTGTGCCATCATCATAAAG-3'

The PCR was performed in a Gene Amp® PCR 2200 thermocycler (Applied Biosystems, USA). The PCR was carried out in 50 µL using 0.3 µM forward and reverse primer, 0.2 mM dNTP-mix, 3.6 U Pfu DNA Polymerase (Promega, USA) and 1x reaction buffer provided by the supplier. The two-stage protocol involved in the first step two separate PCR reactions with the forward and reverse primers. These reactions consisted of a preheating step at 95°C for 60 s followed by 4 reaction cycles (95°C, 50 s; 55°C, 50 s; 70°C, 10 min). After this first step both PCR reactions were mixed together in a 1:1 ratio followed by second standard mutagenesis PCR reaction using the same temperature program (95°C, 50 s; 55°C, 50 s; 70°C, 10 min) for 18 cycles. The amplification product was subjected to parental template digest by *Dpn*I (Fermentas, Germany) in accordance to the manufacturer's instructions and transformed into electro-competent *E. coli* BL21_Gold(DE3) cells. All inserts were sequenced as custom service by Agowa (Germany). Wizard® Plus SV Minipreps Kit from Promega (USA) was used to prepare plasmid DNA. DNA analysis was performed with Vector NTI Suite 10 (Invitrogen, USA).

Protein expression and purification

Protein expression in *E. coli* and preparation of the cell lysate were done as previously described.[2] Target proteins were purified via their C-terminal His-tag using an ÄKTAprime plus system (GE Healthcare, Germany). The cleared cell lysate was

loaded onto two HisTrap HP FF 5 mL columns (GE Healthcare, Germany) at a flow rate of 2 mL min^{-1}. The columns had been equilibrated with binding buffer (30 mM potassium phosphate, 300 mM NaCl, 15 mM imidazol, 10% glycerol, pH 7.4). After a washing step of 10 column volumes, the enzyme was eluted with a linear gradient of 15 - 300 mM imidazol within 10 column volumes. Fractions of 3 mL were collected and analyzed by SDS-PAGE. Sialyltransferase containing fractions were pooled and dialyzed overnight against 20 mM Tris/HCl, 150 mM NaCl, pH 7.5. SDS PAGE was used to confirm purity of enzyme preparations. ~25 mg of each protein (wild-type, P7H, P7H-M117A) were recovered from 1 L bacterial culture after purification. Purified enzymes were aliquoted and stored at -70°C.

Sialyltransferase assay using lactose and *N*-acetyllactosamine as acceptor substrates

Sialyltransferase activity was assayed in a total volume of 20 µL using 50 mM sodium phosphate buffer, pH 8.0. Reaction mixture contained 1 mM CMP-Neu5Ac, 1 mM lactose or *N*-acetyllactosamine, 1 µM enzyme, and 1 mg mL^{-1} BSA. Enzymatic conversion was carried out at 25°C and agitation rate of 400 rpm using a Thermomixer comfort (Eppendorf, Germany). All assays were performed in duplicate. Reactions were stopped after 30 min by adding 40 µL of ice-cold acetonitrile. Mixtures were incubated on ice for 10 min and centrifuged at 4°C, 13,000 rpm for 10 min to remove precipitated protein. For time course experiments 0.1 µM enzyme was used, under otherwise identical conditions, and reactions were stopped after 0, 15, 30, 60, 90, 180 and 240 min.

HPLC analysis of CMP and CMP-Neu5Ac

For CMP and CMP-Neu5Ac analysis 5 µL supernatant were injected after appropriate dilution in HPLC analysis using a Chromolith® HighResolution RP-18 (100 x 4.6 mm; Merck Chemicals, Germany) column in reversed phase ion-pairing mode on an Agilent Technologies 1200 Series system. The column was equilibrated with 20 mM phosphate buffer, pH 6.8 containing 2 mM tetrabutylammonium at a flow rate of 2 mL min^{-1}. A temperature control unit maintained 30°C throughout the analysis. Samples were eluted with a linear gradient from 0 – 2% acetonitrile in 3 min followed by 2 – 25% acetonitrile in 7 min and detected by UV at 254 nm.

Sialyllactose and sialyl-*N*-acetyllactosamine analysis

The sialyltransferase assay products (3'- and/or 6'-sialyllactose; 3'- and/or 6'-sialyl-*N*-acetyllactosamine) were identified by HPAE chromatography on a Dionex BioLC system equipped with a CarboPac® PA200 column (3 x 250 mm; Thermo Fisher Scientific Inc., Dionex) and a CarboPac® guard column. After appropriate dilution of the supernatant 25 µL were injected and eluted using an isocratic concentration of 60 mM NaOH with 35 mM sodium acetate at a flow rate of 0.4 mL min^{-1} at 25°C. An ED50 electrochemical detector with a carbohydrate certified gold working electrode was used for pulsed amperometric detection (PAD) in the carbohydrate waveform (as recommended by the supplier).

One unit (1 U) was defined as the amount of enzyme that could transfer 1 µmol of sialic acid per min to lactose under the conditions described above.

Identification of sialyltransferase assay products by NMR

The α2,3- and α2,6-regioselectivity of sialyltransferase assay products (3'- or 6'-sialyllactose and 3'- or 6'-sialyl-*N*-acetyllactosamine) was proven by NMR spectroscopy. ^{1}H NMR (500 MHz) spectra were recorded on a Varian INOVA 500 MHz spectrometer (Agilent Technologies, Santa Clara United States) equipped with a 5 mm indirect detection probe. 4.8 mL scale reactions were carried out. For reaction conditions see 'Sialyltransferase assay using lactose and *N*-acetyllactosamine as acceptor substrates'. After enzyme and BSA removal by Vivaspin centrifugal concentrators (MWCO 10 kDa, Sartorius, Germany) at 5000 rpm and 4°C, samples were frozen and freeze-dried. Commercial standards (3'- and 6'-sialyllactose; 3'- and 6'-sialyl-*N*-acetyllactosamine) from Carbosynth (UK) and the product mixtures after wild-type PdST and P7H-M117A double mutant catalyzed conversion were dissolved in D_2O and ^{1}H spectra were recorded with presaturation of the residual water signal. The HSQC spectra were measured with 128 scans per increment and adiabatic carbon 180° pulses. Product identity was unequivocally confirmed by overlay of NMR spectra (^{1}H, HSQC) of commercial standards (3'- and 6'-sialyllactose; 3'- and 6'-sialyl-*N*-acetyllactosamine) and PdST (wild-type, P7H-M117A) catalyzed conversions, showing exact match of main peaks.

Kinetic characterization

To obtain the kinetic parameters of lactose as acceptor substrate for sialyltransferase activity, initial rate measurements were performed in duplicate in a total volume of 20 µL using 50 mM sodium phosphate buffer, pH 8.0. Incubations were done at 25°C using agitation at 400 rpm on a Thermomixer comfort (Eppendorf, Germany). Reaction mixture contained a fixed concentration of CMP-Neu5Ac (10 mM), different

concentrations of lactose (0.25 - 30 mM), 1 mg mL^{-1} BSA and 0.1 µM of PdST enzymes (wild-type, M117A, P7H, P7H-M117A). Reactions were stopped after certain time points by adding 40 µL of ice-cold acetonitrile. Mixtures were incubated on ice for 10 min and centrifuged at 4°C, 13,000 rpm for 10 min to remove precipitated protein. 3'- and/or 6'-sialyllactose concentration was measured by HPAE chromatography as described for sialyllactose and sialyl-*N*-acetyllactosamine analysis. Apparent kinetic parameters were obtained from non-linear least squares fits (SigmaPlot, Systat, Germany) of initial rates to the Michaelis-Menten equation.

Crystallization and structure determination

For the crystallization setups the proteins were concentrated using Amicon Ultra Centrifugal Filters (Ultracel-10K, Millipore) and the concentrations were determined using NanoDrop (Thermo Scientific). The crystallization experiments of wild-type, P7H and P7H-M117A variants were set up with the vapor diffusion method using an Oryx-8 robot (Douglas Instruments) and Index (Hampton Research) as well as JCSG+ (Molecular Dimensions) screens. Crystallization trials of P7H and P7H-M117A were set up also in the presence of CMP-Neu5Ac (2 mM final concentration) and lactose or 2-nitrophenyl-β-D-galactopyranoside (oNP-Gal) (5 mM final concentration). The total drop volume was 1 µL containing 50% of the protein and 50% of the reservoir solution. Protein concentrations used for crystallization setups were 3.3 mg mL^{-1} for wild-type, 5.2 mg mL^{-1} for the P7H and 6.7 mg mL^{-1} for the P7H-M117A (10 mM Tris/HCl pH 8.0, 50 mM NaCl) variant. Crystallization plates were kept in the incubator at 16°C. Crystals appeared after 3 days in several conditions. Small amounts of glycerol were added to the drops and the crystals were pulled out of the drops with a nylon loop and were immediately flash-cooled in liquid

nitrogen. Additionally, the same crystals were soaked with an excess of lactose/oNP-Gal for a 30 min – 1 h period before flash-cooling in liquid nitrogen. Diffraction data were collected at 100K using synchrotron radiation provided by DESY (PETRA III, Hamburg, Germany) and ESRF (Grenoble, France).[3] Data were processed, merged and scaled using the XDS programs.[4] The R_{free} column comprising a randomly selected 5% of the reflections was introduced. Data collection, phasing and refinement statistics can be found in Table S2. The structures were solved by molecular replacement using the program Phaser.[5] The structure of sialyltransferase Pm0188 from *Pasteurella multocida* (PDB code 2ILV)[6] was used as the template for solving the apo structure of wild-type PdST. For all other structures the wild-type structure or its N- and C-terminal domains were used as the initial phasing model. Refinement and manual model rebuilding were carried out with REFMAC5[7] and Coot[8] and concluded when no significant changes in R_{work} and R_{free} were observed. The validation of the final structures was performed with MolProbity.[9]

Crystals of wild-type PdST were obtained in the Index screen condition D9 (0.1 M Tris pH 8.5, 25% w/v Polyethylene glycol 3350). Crystals of the P7H and P7H-M117A variants were obtained in JCSG-plus screen conditions G7 (0.1 M succinic acid, 15% w/v PEG 3350, pH 7.0) and B9 (0.1 M citrate, 20% w/v PEG 6000, pH 5.0). Structures of the P7H and P7H-M117A variants in the closed conformation with bound CMP were determined from crystals obtained by co-crystallization and soaking experiments with CMP-Neu5Ac and lactose or oNP-Gal. Data were collected on P7H and P7H-M117A crystals grown in JCSG-plus screen conditions A9 (0.2 M ammonium chloride, 20% w/v PEG 3350), A2 (0.1 M sodium citrate, 20% w/v PEG 3000, pH 5.5), A5 (0.2 M magnesium formate, 20% w/v PEG 3350) and A12 (0.2 M potassium nitrate, 20% w/v PEG 3350). No residual electron density for lactose or

oNP-Gal could be observed.

Since no apo structure of the α2,6-sialyltransferase from *Photobacterium* sp. JT-ISH-224 is available for comparison, we divided the deposited structure of the enzyme in complex with CMP and lactose (PDB code 2Z4T)[10] into two domains: an N-terminal (residues 22 - 338) and a C-terminal (residues 339 - 514) domain. Both domains were superimposed individually to the structure of the P7H-M117A variant using SSM superposition[11] as included in Coot [8] (Fig. S15).

Table S1. Partial sequence alignment displaying differences among α2,3- and α2,6-STs in GT family 80.

	Sialyltransferase	Acceptor	Accession number	⬇	⬇
P. dagmatis	α2/3	β	AFY98851	TIYLDP^{7} ASLPT	YDDGTM^{117}EYVDL
P. multocida	α2,3/α2,6	β	AAY89061	TLYLDP^{34} ASLPA	YDDGSM^{144}EYVDL
P. phosphoreum	α2,3	α/β	BAF63530	EVYVDR^{47} ATLPT	YDDGSA^{151}EYVRL
Vibrio sp.	α2,3	α/β	BAF91160	EIYVDR^{41} ATLPT	YDDGSA^{145}EYVRI
Photobacterium sp. JT-ISH-224	α2,3	α/β	BAF92025	EVYVDR^{47} ATLPT	YDDGSA^{151}EYVRL
H. ducreyi	α2,3	-	AAP95068	EIYLDY^{13} ATIPS	YDDGSE^{128}GIVTQ
Photobacterium sp. JT-ISH-224	α2,6	β	BAF92026	EVYVDH^{123}ASLPT	YDDGSA^{235}EYVNL
P. damselae	α2,6	β	BAA25316	EVYIDH^{120}ASLPS	YDDGSS^{232}EYVSL
P. leiognathi JT-SHIZ-145	α2,6	β	BAF91416	EVYVDH^{120}ASLPS	YDDGSA^{232}EYVSL
P. leiognathi JT-SHIZ-119	α2,6	β	BAI49484	EVYVDH^{120}ASLPS	YDDGSA^{232}EYVNL

P. dagmatis, *Pasteurella dagmatis* β-galactoside α2,3-sialyltransferase (PdST); *P. multocida*, *Pasteurella multocida* β-galactoside α2,3/α2,6-sialyltransferase (PmST1); *P. phosphoreum*, *Photobacterium phosphoreum* α/β-galactoside α2,3-sialyltransferase; *Vibrio* sp., *Vibrio* sp. α/β-galactoside α2,3-sialyltransferase; *Photobacterium* sp., *Photobacterium* sp. α/β-galactoside α2,3-sialyltransferase; *H. ducreyi*, *Haemophilus ducreyi* α2,3-sialyltransferase; *Photobacterium* sp., *Photobacterium* sp. β-galactoside α2,6-sialyltransferase; *P. damselae*, *Photobacterium damselae* β-galactoside α2,6-sialyltransferase; *P. leiognathi, Photobacterium leiognathi* β-galactoside α2,6-sialyltransferase. Sequence alignment was performed with ClustalW using a blosum scoring matrix and an open gap penalty of 10. Potentially critical amino acids for reaction specificity are indicated by an arrow.

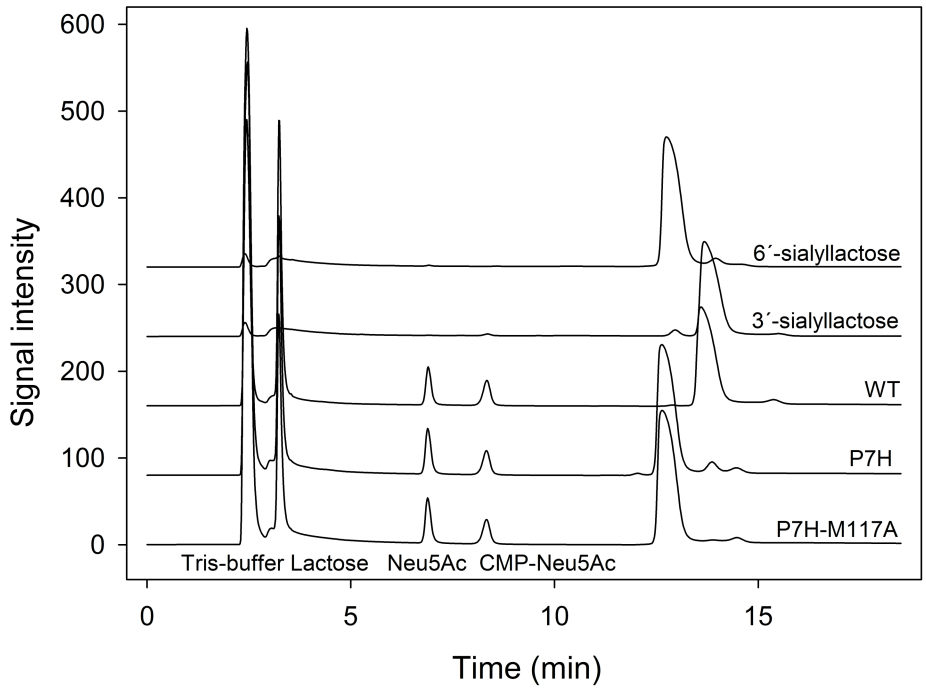

Fig. S1. Gradual change from α2,3- to α2,6-regioselective sialyltransfer from CMP-Neu5Ac to lactose, resulting from substitution of Pro^{7} by His and from additional substitution of Met^{117} by Ala in PdST. Traces of HPAEC-PAD analysis of samples from different enzymatic reactions are superimposed along with traces of authentic 3'- and 6'-sialyllactose standards. The concentration of sialyllactose in each sample was approximately 0.7 mM.

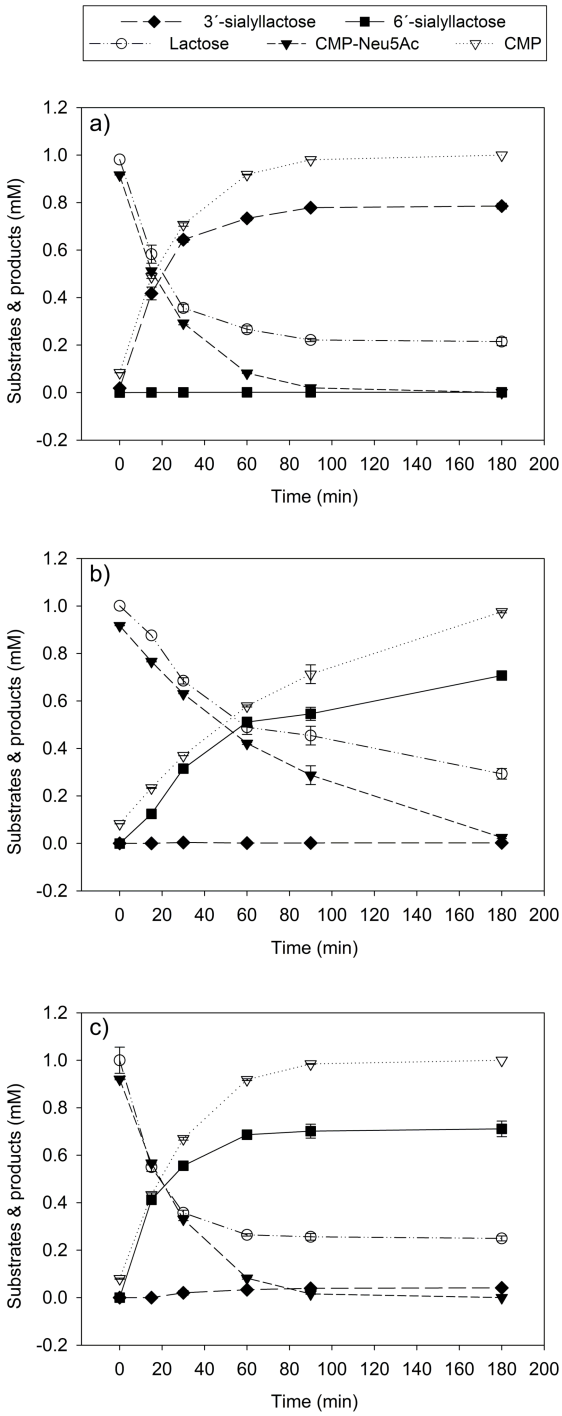

Fig. S2. Time courses of enzymatic synthesis of sialyllactose at pH 8.0 using 0.1 µM wild-type PdST (a), P7H-M117A double (b) and P7H single (c) variant thereof. The reaction mixture (20 µL), containing 1 mM CMP-Neu5Ac, 1 mM lactose, 1 mg mL^{-1} BSA in 50 mM sodium phosphate buffer, pH 8.0 was incubated at 25°C and 400 rpm.

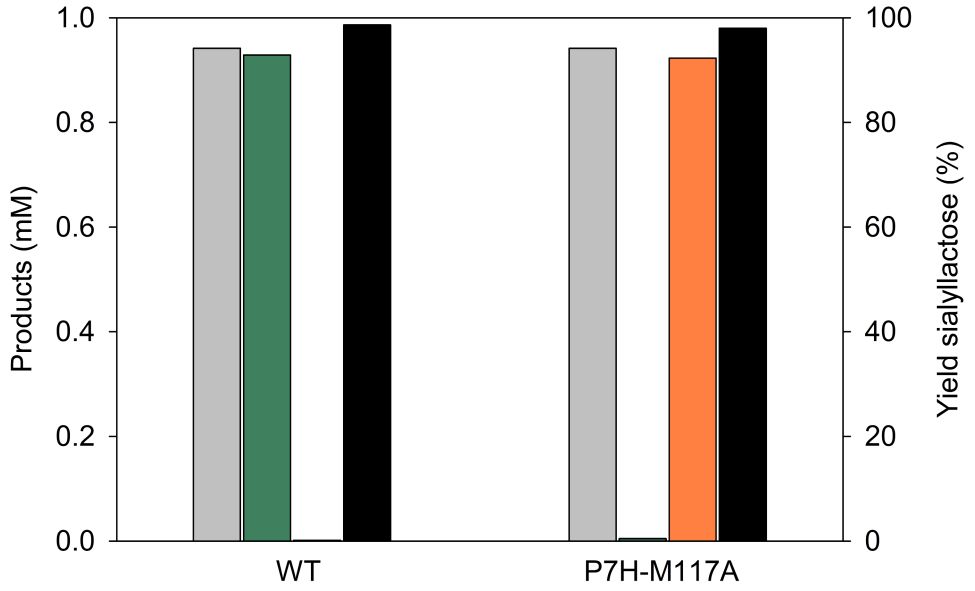

Fig. S3. Concentrations of formed products (CMP, grey bars; 3´-sialyllactose, green bars, 6´-sialyllactose, orange bars) and the corresponding sialyllactose yields (black bars) after complete conversion of CMP-Neu5Ac when lactose was employed in 10-fold molar excess. The reaction mixture, containing 0.94 mM CMP-Neu5Ac, 10 mM lactose, 1 µM enzyme (WT or P7H-M117A), 1 mg mL^{-1} BSA in 50 mM sodium phosphate buffer pH 8.0 was incubated at 25°C and 400 rpm.

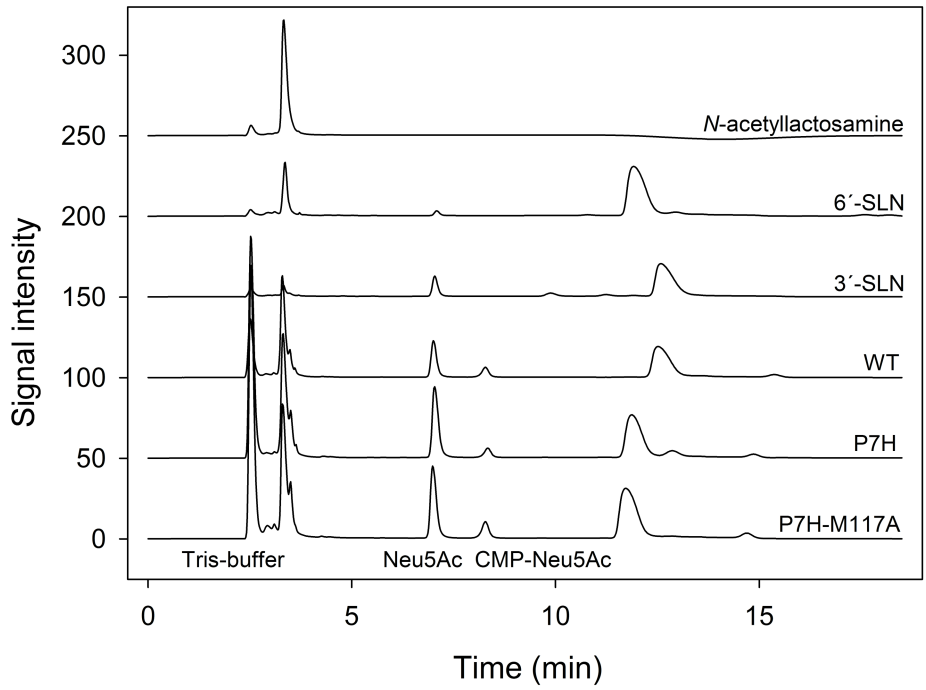

Fig. S4. Gradual change from α2,3- to α2,6-regioselective sialyltransfer from CMP-Neu5Ac to *N*-acetyllactosamine, resulting from substitution of Pro^{7} by His and from additional substitution of Met^{117} by Ala in PdST. Traces of HPAEC-PAD analysis of samples from different enzymatic reactions are superimposed along with traces of authentic *N*-acetyllactosamine, 3'- and 6'-sialyl-*N*-acetyllactosamine (3'- and 6'-SLN) standards.

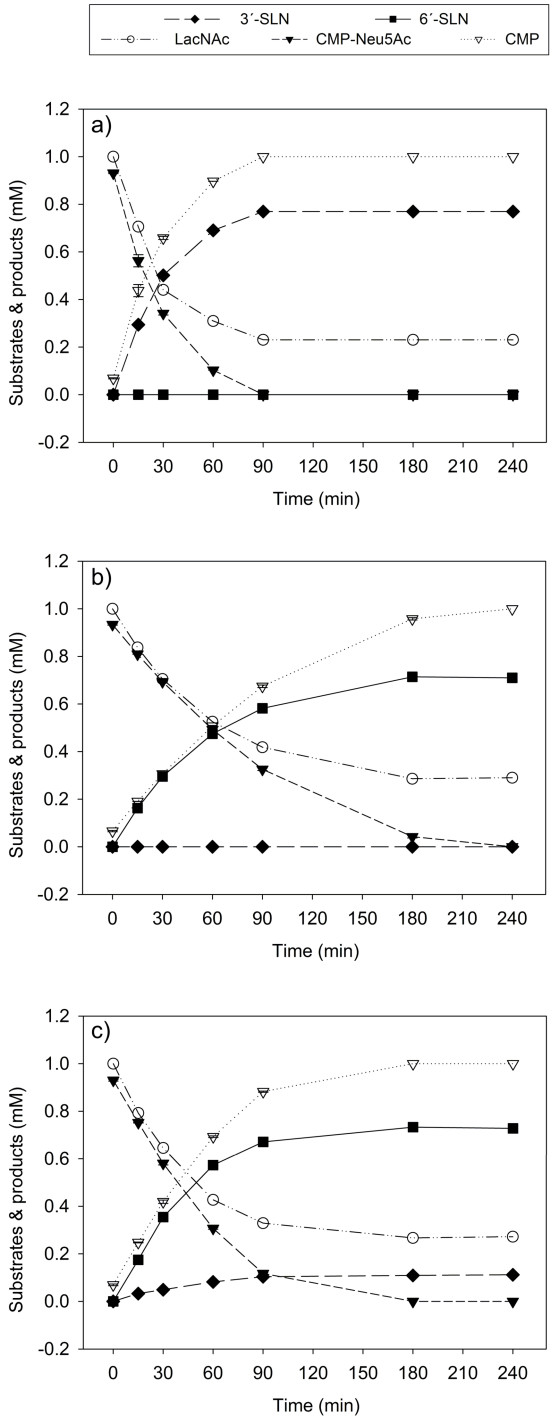

Fig. S5. Time courses of enzymatic synthesis of sialyl-*N*-acetyllactosamine at pH 8.0 using 0.1 µM wild-type PdST (a), P7H-M117A double (b) and P7H single (c) variant thereof. LacNAc, *N*-acetyllactosamine; 3'- and 6'-SLN, 3'- and 6'-sialyl-*N*-acetyllactosamine. The reaction mixture (20 µL), containing 1 mM CMP-Neu5Ac, 1 mM LacNAc, 1 mg mL^{-1} BSA in 50 mM sodium phosphate buffer, pH 8.0 was incubated at 25°C and 400 rpm.

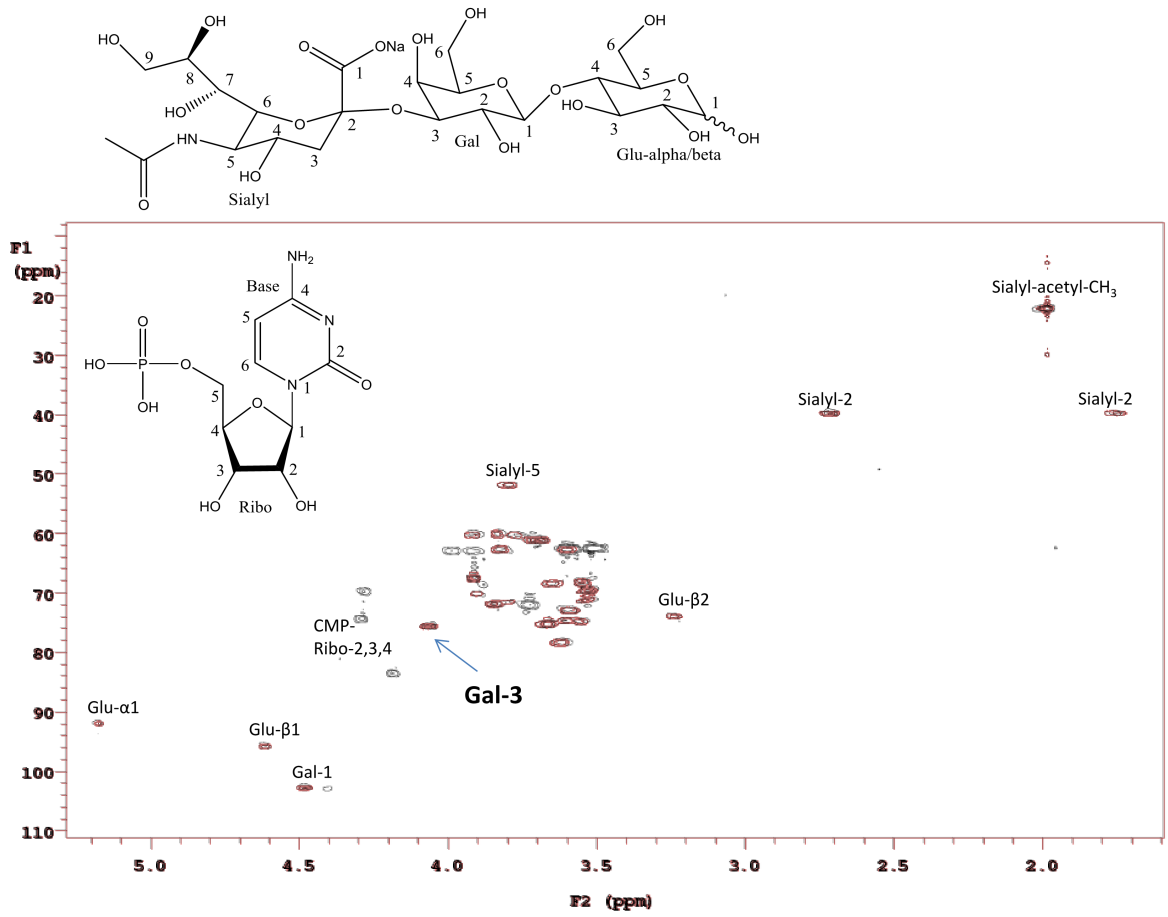

Fig. S6. Overlay of HSQC NMR (500 MHz) spectra of commercial 3'-sialyllactose standard in red and wild-type PdST catalyzed conversion using lactose as acceptor substrate in black (contains also CMP). Standard and reaction mixture were dissolved in D_2O. Only characteristic peaks are assigned for clarity. Main peaks of commercial standard and enzymatic conversion match exactly.

.

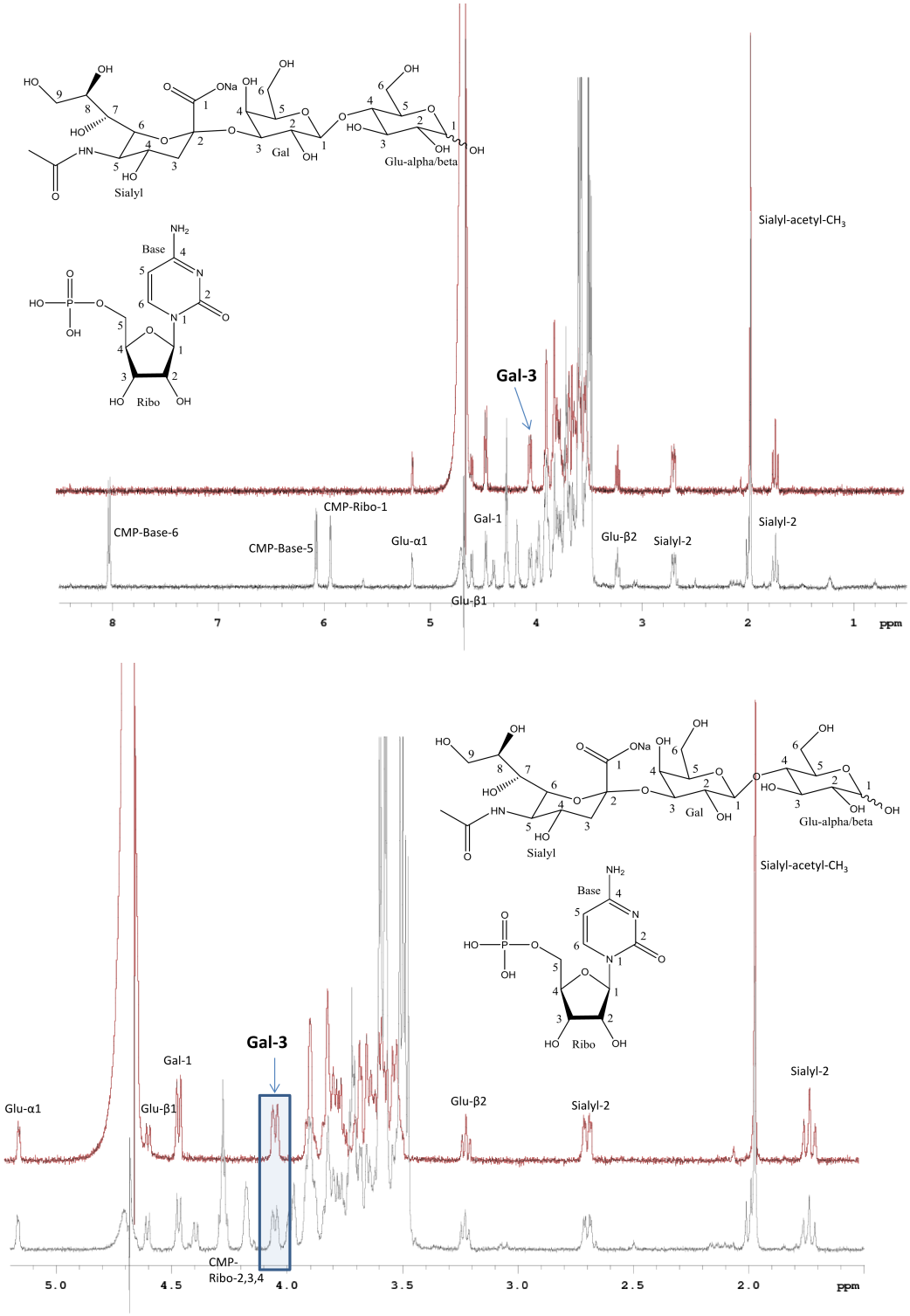

Fig. S7. Overlay of ^{1}H NMR (500 MHz) spectra of commercial 3'-sialyllactose standard in red and wild-type PdST catalyzed conversion using lactose as acceptor substrate in black (contains also CMP). Standard and reaction mixture were dissolved in D_2O. Only characteristic peaks are assigned for clarity. Main peaks of commercial standard and enzymatic conversion match exactly.

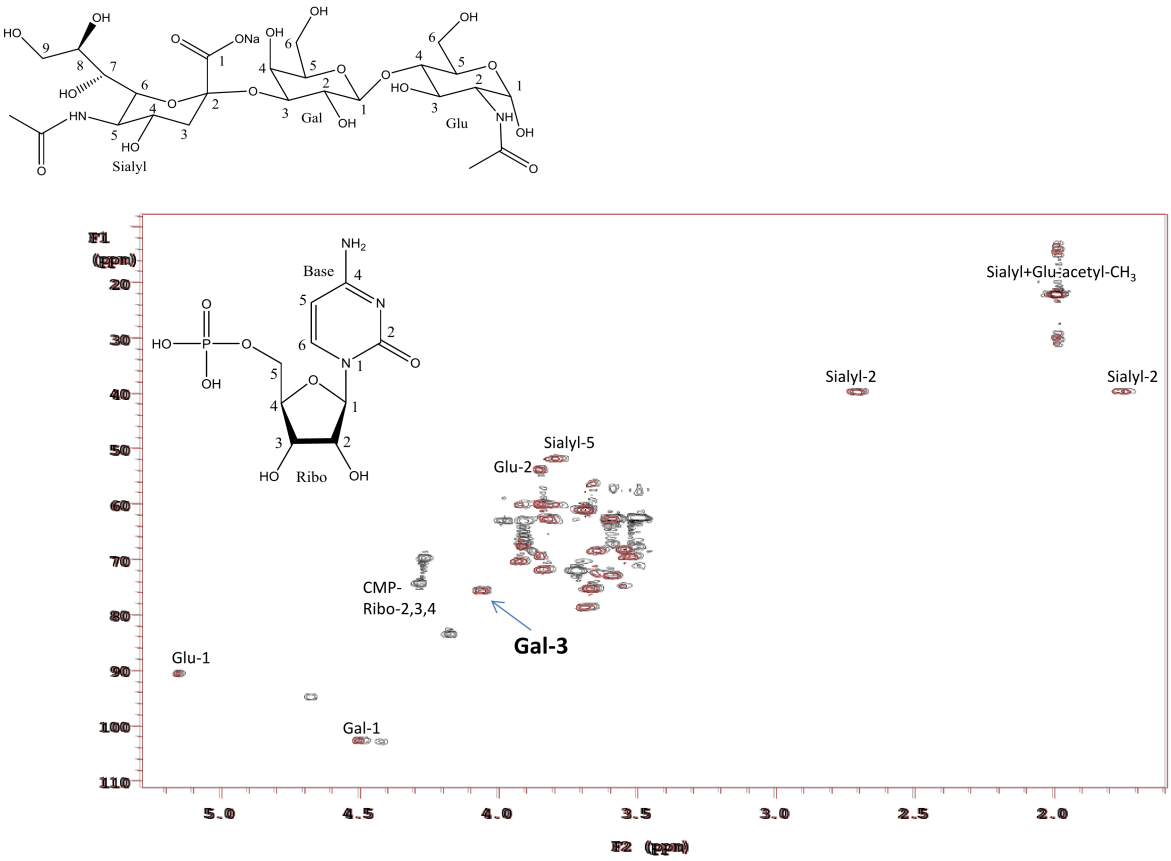

Fig. S8. Overlay of HSQC NMR (500 MHz) spectra of commercial 3'-sialyl-*N*-acetyllactosamine standard in red and wild-type PdST catalyzed conversion using *N*-acetyllactosamine as acceptor substrate in black (contains also CMP). Standard and reaction mixture were dissolved in D_2O. Only characteristic peaks are assigned for clarity. Main peaks of commercial standard and enzymatic conversion match exactly.

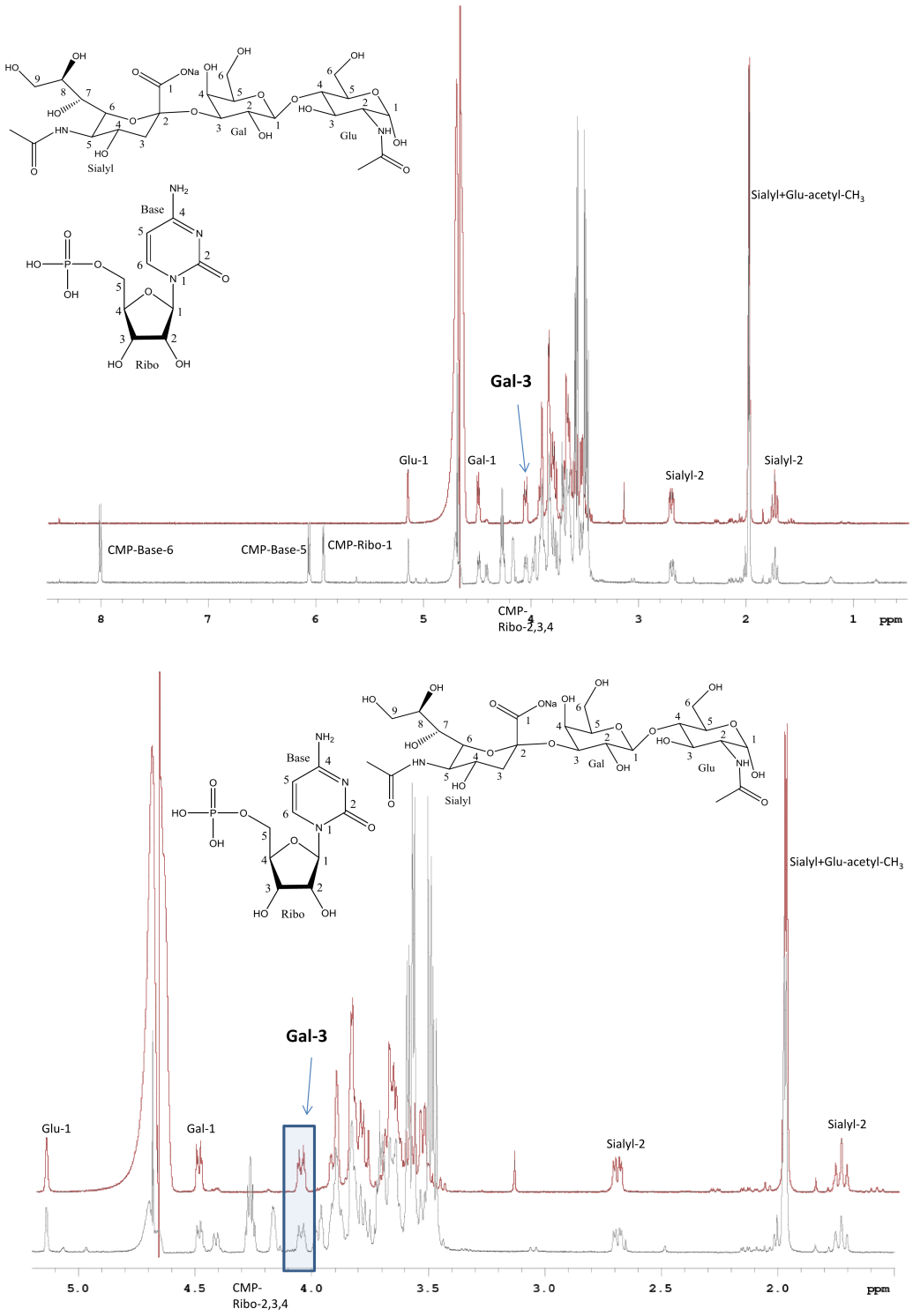

Fig. S9. Overlay of ^{1}H NMR (500 MHz) spectra of commercial 3'-sialyl-*N*-acetyllactosamine standard in red and wild-type PdST catalyzed conversion using *N*-acetyllactosamine as acceptor substrate in black (contains also CMP). Standard and reaction mixture were dissolved in D_2O. Only characteristic peaks are assigned for clarity. Main peaks of commercial standard and enzymatic conversion match exactly.

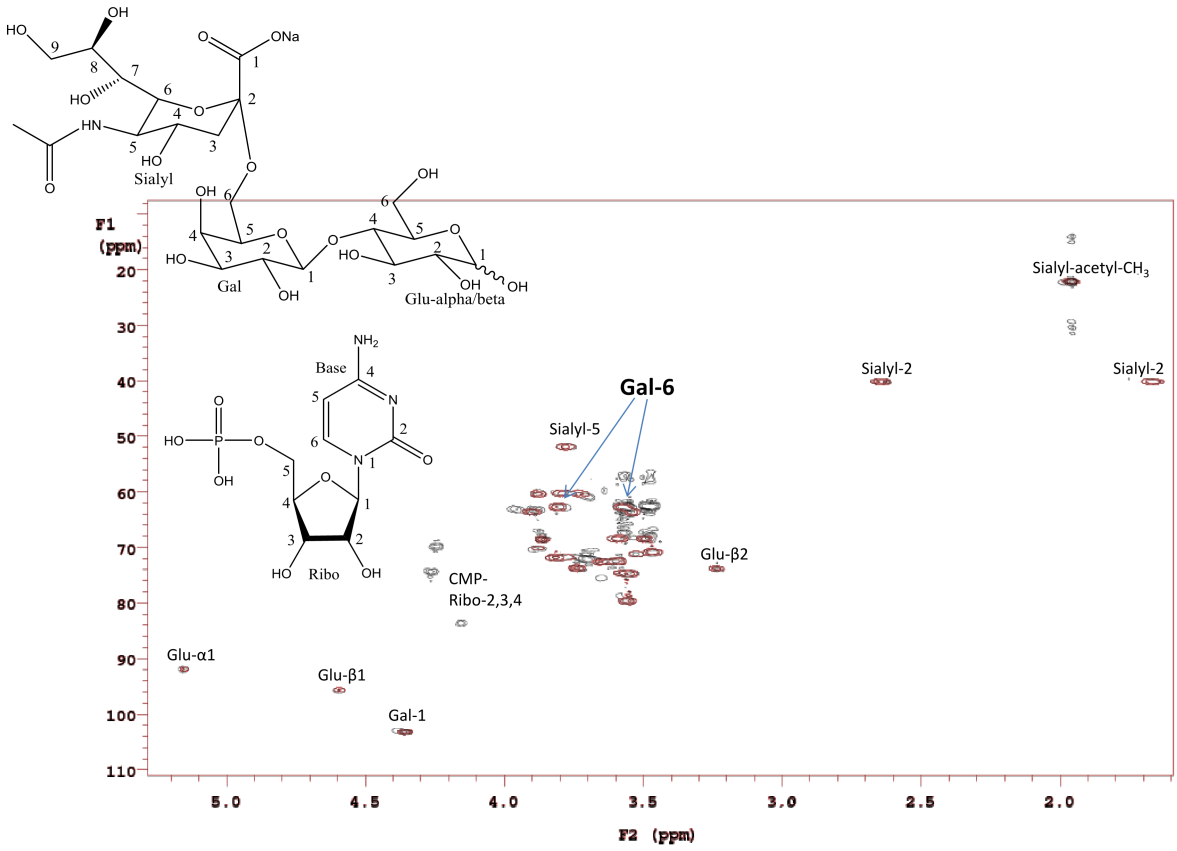

Fig. S10. Overlay of HSQC NMR (500 MHz) spectra of commercial 6'-sialyllactose standard in red and P7H-M117A PdST catalyzed conversion using lactose as acceptor substrate in black (contains also CMP). Standard and reaction mixture were dissolved in D_2O. Only characteristic peaks are assigned for clarity. Main peaks of commercial standard and enzymatic conversion match exactly.

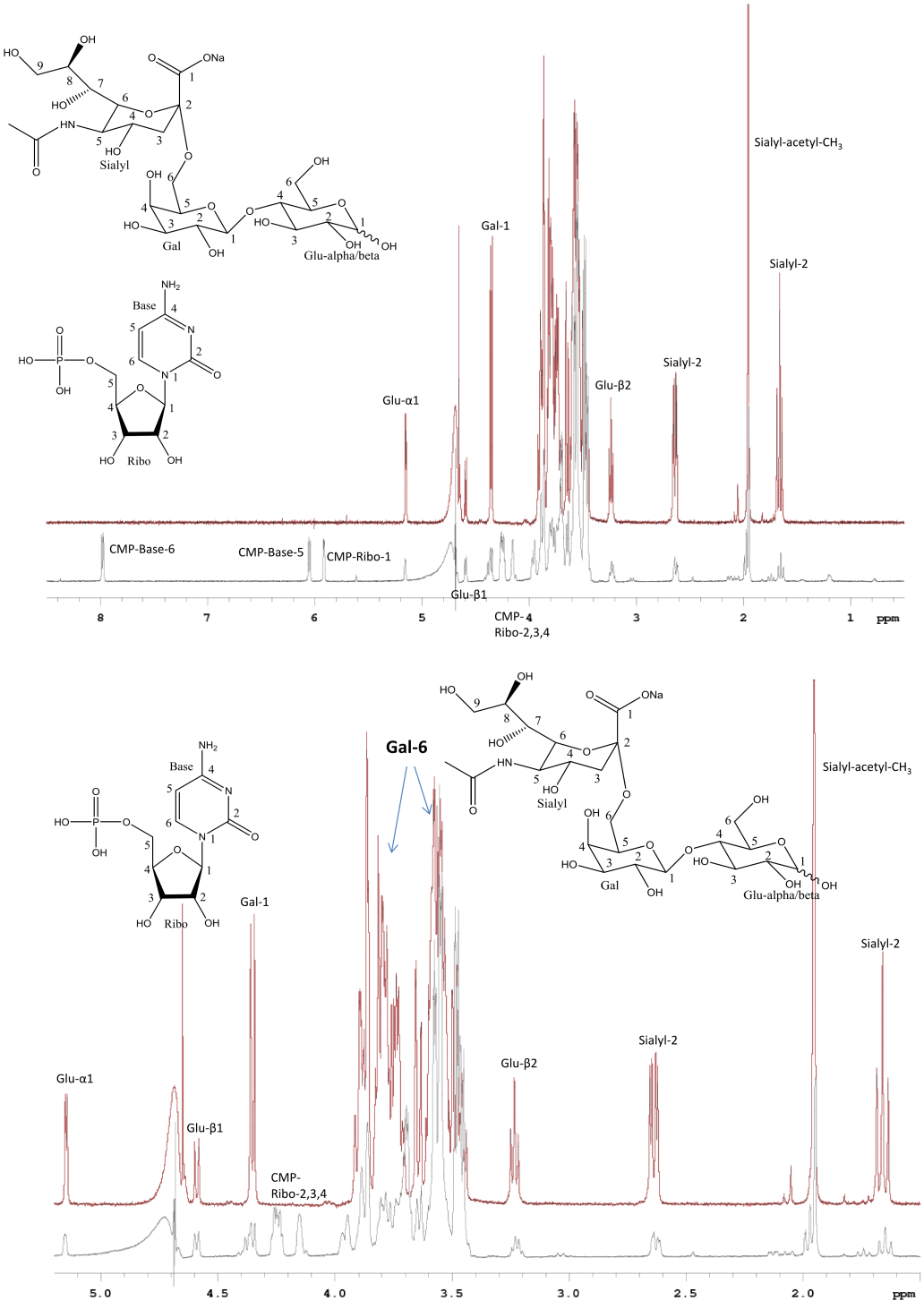

Fig. S11. Overlay of ^{1}H NMR (500 MHz) spectra of commercial 6'-sialyllactose standard in red and P7H-M117A PdST catalyzed conversion using lactose as acceptor substrate in black (contains also CMP). Standard and reaction mixture were dissolved in D_2O. Only characteristic peaks are assigned for clarity. Main peaks of commercial standard and enzymatic conversion match exactly.

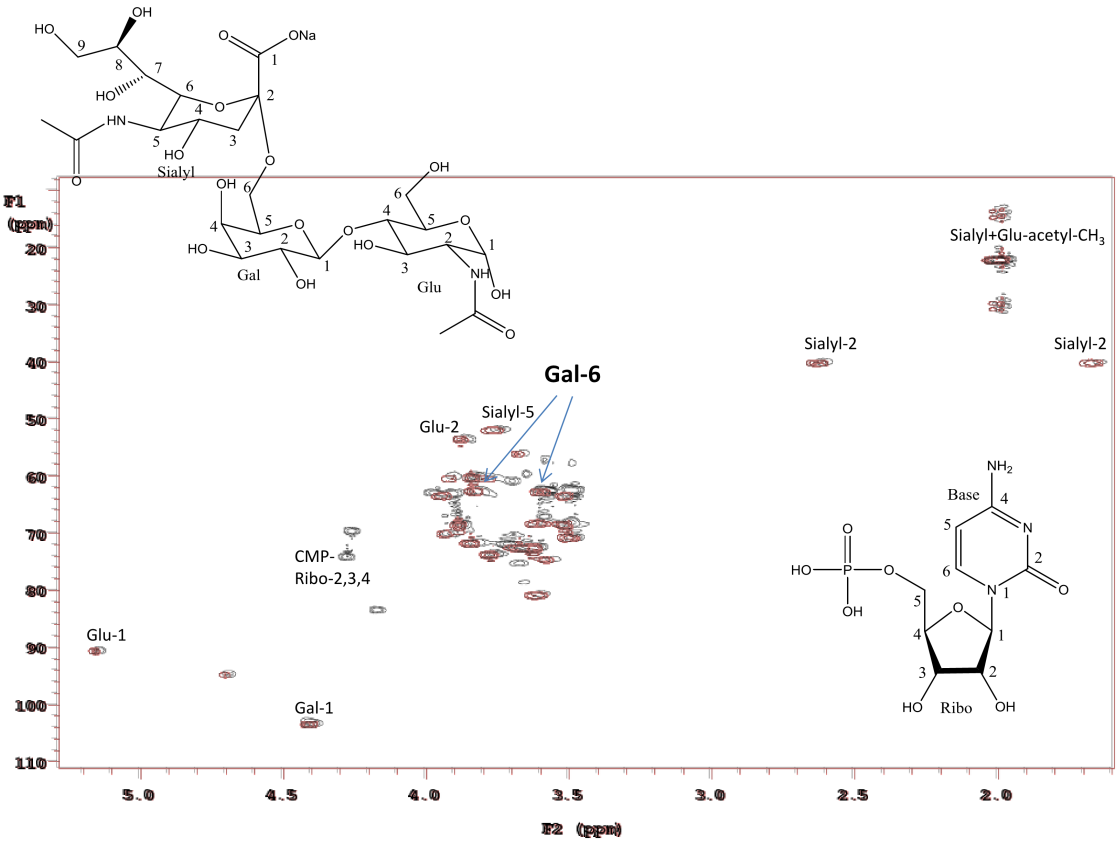

Fig. S12. Overlay of HSQC NMR (500 MHz) spectra of commercial 6'-sialyl-*N*-acetyllactosamine standard in red and P7H-M117A PdST catalyzed conversion using *N*-acetyllactosamine as acceptor substrate in black (contains also CMP). Standard and reaction mixture were dissolved in D_2O. Only characteristic peaks are assigned for clarity. Main peaks of commercial standard and enzymatic conversion match exactly.

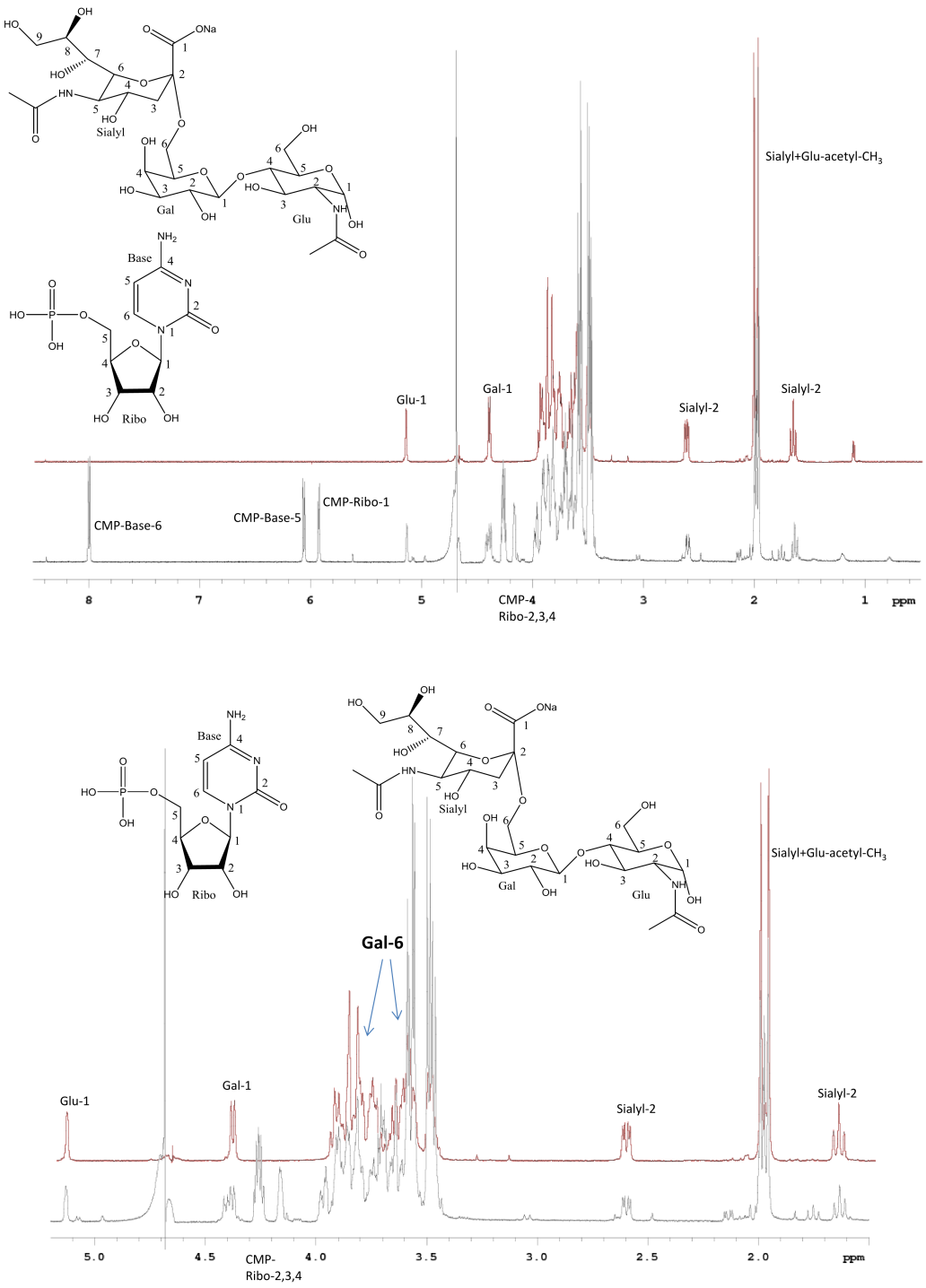

Fig. S13. Overlay of ^{1}H NMR (500 MHz) spectra of commercial 6'-sialyl-*N*-acetyllactosamine standard in red and P7H-M117A PdST catalyzed conversion using *N*-acetyllactosamine as acceptor substrate in black (contains also CMP). Standard and reaction mixture were dissolved in D_2O. Only characteristic peaks are assigned for clarity. Main peaks of commercial standard and enzymatic conversion match exactly.

Table S2. X-ray data collection and refinement statistics.

	Wild-type	**P7H**	**P7H + CMP**	**P7H-M117A**	**P7H-M117A + CMP**
Data collection					
Beamline	DESY P11	ESRF ID29	ESRF ID23-2	ESRF ID29	ESRF ID29
Wavelength	1.0332	0.9791	0.8726	0.9791	0.9791
Space group	C2	C2	$P6_5$	C2	$P6_5$
a, b, c (Å)	111.7, 56.6, 79.5	112.2, 57.1, 80.2	113.6, 113.6, 65.7	111.2, 56.9, 79.7	111.8, 111.8, 65.2
α, β, γ (°)	90, 111.9, 90	90, 111.4, 90	90, 90, 120	90, 111.4, 90	90, 90, 120
Resolution (Å)[a]	45.1 -2.71 (2.87-2.71)	75-1.83 (1.9-1.83)	50-2.18 (2.26-2.18)	52.3-2.34 (2.52-2.34)	96-1.84 (1.92-1.84)
Rmerge[a]	0.11 (0.63)	0.06 (0.81)	0.09 (0.89)	0.13 (0.81)	0.06 (0.77)
I/σ(I)[a]	10.4 (1.9)	11.9 (1.4)	9.5 (1.2)	10.9 (2.1)	18.8 (1.8)
Completeness (%)[a]	98.8 (97.3)	97.90 (87.3)	99.3 (97.7)	99.2 (99.4)	99.5 (99.6)
Multiplicity[a]	3.3 (3.2)	4.7 (3.6)	3.2 (3.0)	4.8 (4.9)	7.7 (7.8)
Unique reflections	12618	40997	25784	22648	44015
Refinement					
Resolution (Å)	45.1-2.71	75-1.96	50-2.18	52.3-2.60	96-1.84
R_{work}/R_{free}	0.186/0.261	0.190/0.244	0.186/0.238	0.191/0.263	0.170/0.219
R.m.s.d. stereochemistry					
Bond lengths (Å)	0.014	0.013	0.014	0.010	0.014
Bond angles (°)	1.65	1.54	1.68	1.31	1.68
No. of protein atoms	3218	3373	3512	3277	3566
No. of waters	11	127	240	42	297
Average *B* factor ($Å^2$)	46.3	43.8	47.6	36.9	41.1
Ramachandran favored (%)	95	97	97	96	98
Ramachandran outliers (%)	0	0	0	0.5	0
PDB code	4V2U	4V38	4V3B	4V39	4V3C

[a] Values in parentheses refer to the outer resolution shell

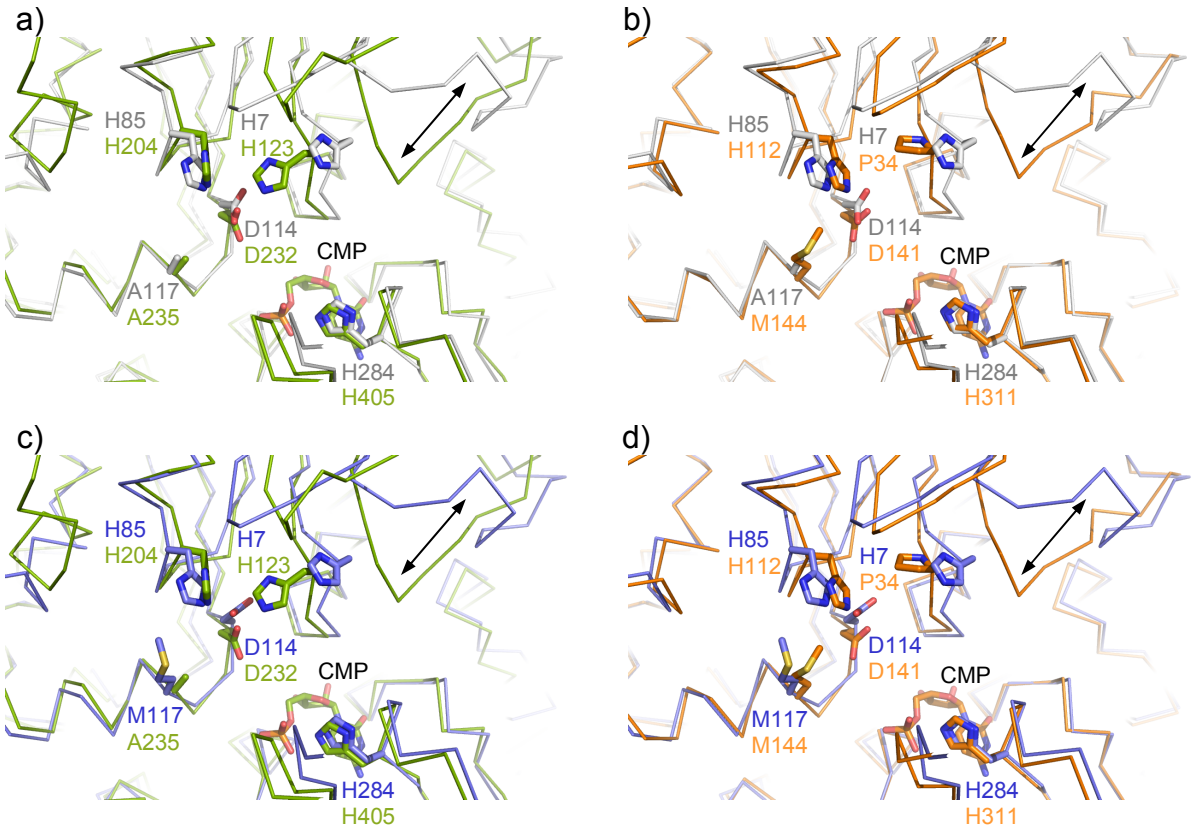

Fig. S14. Superposition between binary CMP-bound structures of PdST variants and ternary sialyltransferase structures (with CMP plus lactose bound) of *Photobacterium* sp.[10] and *Pasteurella multocida*.[6] Overlay of P7H-M117A double mutant (grey, PDB code 4V3C) and α2,6-sialyltransferase from *Photobacterium* sp. JT-ISH-224 (green, PDB code 2Z4T)[10] (a) and α2,3/α2,6-sialyltransferase from *P. multocida* (PmST1) (orange, PDB code 2ILV)[6] (b). Overlay of P7H single mutant (blue, PDB code 4V3B) and α2,6-sialyltransferase from *Photobacterium* sp. JT-ISH-224 (green, PDB code 2Z4T)[10] (c) and α2,3/α2,6-sialyltransferase from *P. multocida* (PmST1) (orange, PDB code 2ILV)[6] (d). Key active-site residues (Asp^{114}/Asp^{232}/Asp^{141}, His^{284}/His^{405}/His^{311})[6,10,12], mutation sites (His^{7}/His^{123}/Pro^{34}, Ala^{117}/Ala^{235}/Met^{144}) and other selected active site residues (His^{85}/His^{204}/His^{112}) involved in lactose binding[6,10] are drawn in sticks. Positions of CMP (only one molecule shown for better clarity; drawn with green- and orange-colored carbon atoms, respectively) and active-site residues are overlapping. Only the loop region Phe^{34}-Lys^{38} (residue numbering of PdST) displays a higher flexibility, indicated by a double-headed arrow.

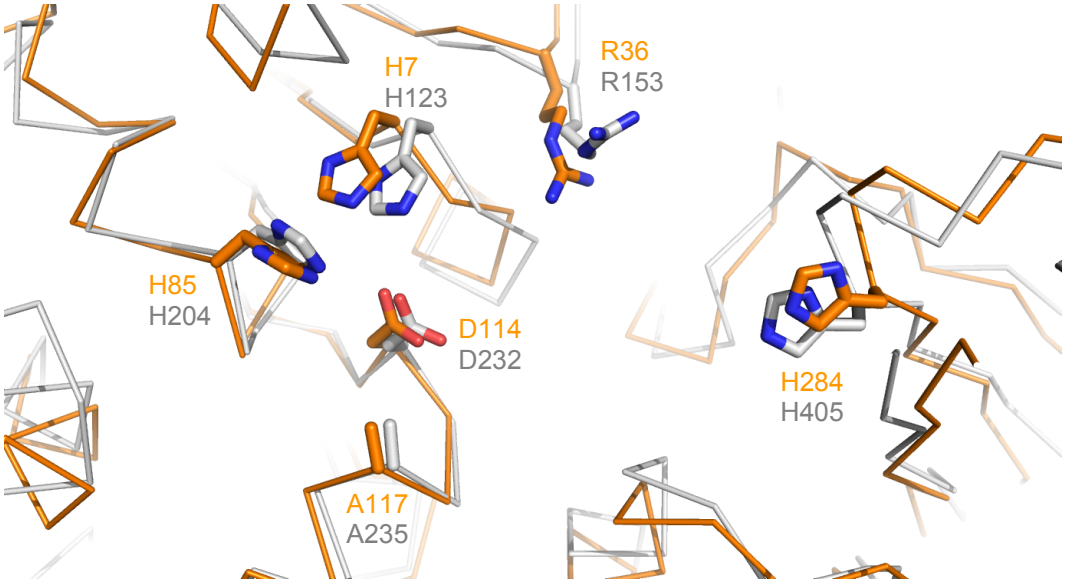

Fig. S15. Overlay of apo structure of PdST P7H-M117A double mutant (orange, PDB code 4V39) with the N- and C-terminal domains of *Photobacterium* sp. α2,6-sialyltransferase (grey, PDB code 2Z4T).[10] For details see Materials and methods in the Supporting Information. Lactose and CMP are omitted for clarity in the ternary *Photobacterium* sp. α2,6-sialyltransferase structure. Key active-site residues (Asp^{114}/Asp^{232}, His^{284}/His^{405})[6,10,12], mutation sites (His^{7}/His^{123}, Ala^{117}/Ala^{235}) and other selected active site residues (His^{85}/His^{204}; Arg^{36}/Arg^{153} located on flexible loop region see Fig. S14) involved in substrate binding[6,10] are drawn in sticks.

References for Supporting Information

1 W. Wang and B. A. Malcolm, *BioTechniques*, 1999, **26**, 680.

2 K. Schmölzer, D. Ribitsch, T. Czabany, C. Luley-Goedl, D. Kokot, A. Lyskowski, S. Zitzenbacher, H. Schwab and B. Nidetzky, *Glycobiology*, 2013, **23**, 1293.

3 (a) D. de Sanctis, A. Beteva, H. Caserotto, F. Dobias, J. Gabadinho, T. Giraud, A. Gobbo, M. Guijarro, M. Lentini, B. Lavault, T. Mairs, S. McSweeney, S. Petitdemange, V. Rey-Bakaikoa, J. Surr, P. Theveneau, G. A. Leonard and C. Mueller-Dieckmann, *J. Synchrotron Radiat.*, 2012, **19**, 455; (b) D. Flot, T. Mairs, T. Giraud, M. Guijarro, M. Lesourd, V. Rey, D. van Brussel, C. Morawe, C. Borel, O. Hignette, J. Chavanne, D. Nurizzo, S. McSweeney and E. Mitchell, *J. Synchrotron Radiat.*, 2010, **17**, 107.

4 W. Kabsch, *Acta Crystallogr D Biol Crystallogr*, 2010, **66**, 125.

5 A. J. McCoy, R. W. Grosse-Kunstleve, P. D. Adams, M. D. Winn, L. C. Storoni and R. J. Read, *J Appl Crystallogr*, 2007, **40**, 658.

6 L. Ni, H. A. Chokhawala, H. Cao, R. Henning, L. Ng, S. Huang, H. Yu, X. Chen and A. J. Fisher, *Biochemistry*, 2007, **46**, 6288.

7 G. N. Murshudov, P. Skubak, A. A. Lebedev, N. S. Pannu, R. A. Steiner, R. A. Nicholls, M. D. Winn, F. Long and A. A. Vagin, *Acta Crystallogr., Sect. D: Biol. Crystallogr.*, 2011, **67**, 355.

8 P. Emsley, B. Lohkamp, W. G. Scott and K. Cowtan, *Acta Crystallogr D Biol Crystallogr*, 2010, **66**, 486.

9 V. B. Chen, W. B. Arendall, 3rd, J. J. Headd, D. A. Keedy, R. M. Immormino, G. J. Kapral, L. W. Murray, J. S. Richardson and D. C. Richardson, *Acta Crystallogr D Biol Crystallogr*, 2010, **66**, 12.

10 Y. Kakuta, N. Okino, H. Kajiwara, M. Ichikawa, Y. Takakura, M. Ito and T. Yamamoto, *Glycobiology*, 2008, **18**, 66.

11 E. Krissinel and K. Henrick, *Acta Crystallogr., Sect. D: Biol. Crystallogr.*, 2004, **60**, 2256.

12 K. Schmölzer, C. Luley-Goedl, T. Czabany, D. Ribitsch, H. Schwab, H. Weber and B. Nidetzky, *FEBS Lett.*, 2014, **588**, 2978.